A DFT Chemical Descriptor to Predict the Selectivity in α-Olefins in the Catalytic Metallacyclic Oligomerization Reaction of Ethylene According to the (Hemi)labile Ligand Coordinating to Titanium

Theodorus de Bruin,*[,†] Pascal Raybaud,[‡] and Hervé Toulhoat[§]

IFP, Direction Chimie et Physico-Chimie Appliquées, 1 & 4 Avenue de Bois Préau, 92852 Rueil-Malmaison Cedex, France, IFP, Direction Catalyse et Séparation, Rond-point de l'échangeur de Solaize, BP 3 69360 Solaize, France, and IFP, Direction Scientifique, 1 & 4 Avenue de Bois Préau, 92852 Rueil-Malmaison Cedex, France

Received April 11, 2008

Density functional theory (B3LYP functional) has been applied to investigate the role of hemilabile ligands composed of a cyclopentadienyl group tethered to a pendent R-group, which are used in titanium-based catalysts to selectively trimerize ethylene into 1-hexene. In order to fairly compare the influence of the R-group on the reaction outcome, it was assumed in this study that, independent of the nature of the R-group, the catalyst enters the metallacyclic mechanistic pathway. The identified competing reaction pathways that determine the selectivity, i.e., the opening of the seven-membered ring to yield 1-hexene and the uptake and insertion reaction of the fourth ethylene molecule, have been explored for 15 catalytic systems. The theoretical results show that the nature of the R-group hardly affects the energy barrier for the ring-opening reaction. On the other hand, the uptake and insertion reaction of the fourth ethylene molecule is favored by more labile R-groups. The lability of the R-group has been quantified by calculating the dissociation energy, using isodesmic reactions. Correlating the barrier heights of the two competing reaction pathways and taking into account the experimental data of catalysts **1**−**7**, a model is derived that predicts the formation of 1-hexene when the dissociation energy is larger than 15 kcal/mol. In the case of smaller dissociation energies, multiple insertion reactions are likely to occur. Next, the model has been applied to six catalysts (**8**−**13**) and found to correctly predict the major product for five catalysts. The dissociation energy thus appears as a relevant DFT chemical descriptor for the research of new analogous hemilabile ligands. For catalysts **14** and **15**, where no experimental data are available, the model foresees respectively 1-hexene and longer oligomers, resulting from multiple insertion reactions, as the major products.

1. Introduction

Alpha-olefins are popular building blocks for the chemical industry, as they are frequently used as monomers for the production of poly-α-olefins and as co-monomers in catalytic olefin polymerization to manufacture different linear low-density polyethylene grades.[1] Nowadays catalytic systems are known to oligomerize ethylene only to a certain, often well-defined, length of α-olefins, by the use of metallacycles.[2] Such catalytic systems are in sharp contrast to other organometallic catalysts, which generate mixtures of olefins that follow a Schulz−Flory type of distribution and consequently require tedious product separation processes.

These metallacycles are formed by the uptake and insertion of a distinct number of ethylene molecules, and once the metallacycle reaches a certain size, it undergoes a ring-opening reaction to finally yield the α-olefin. It is thus of great interest to control the precise number of inserted ethylene molecules to produce an α-olefin of a certain number of carbon atoms with high purity.

Chart 1

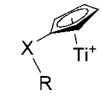

Several examples of such systems can be found in the literature, and some of them are already commercialized.[3] These metallacyclic systems are most often based on chromium,[4] but examples with tantalum[5] or titanium[6] can also be found. For example, the Ti-based catalyst uses a Ti^+ cation in which the oxidation state varies from II or IV during the mechanistic pathway, and where the cyclopentadienyl (Cp) group is connected via a $-C(CH_3)_2-$ bridge to a phenyl group that sandwiches the metal ion. Chart 1 displays the assumed activated bare catalyst after activation by MAO of the precursor η^5-$C_5H_4CMe_2C_6H_5TiCl_3$, in which R = phenyl and X = $-C(CH_3)_2-$. This catalyst shows a high selectivity and activity toward 1-hexene. In fact, the trimerization of ethylene could be realized in about 97% yield with a high selectivity toward 1-hexene (83 wt %) and 14 wt % of C10, which essentially

* To whom correspondence should be addressed. Tel: +33 147525438. Fax: +33 14752 7058. E-mail: theodorus.de-bruin@ifp.fr.
† Direction Chimie et Physico-Chimie Appliquées.
‡ Direction Catalyse et Séparation.
§ Direction Scientifique.

(1) (a) Lappin, G. R.; Nemec, L. H.; Sauer, J. D.; Wagner, J. D. In *Kirk-Othmer Encyclopedia of Chemical Technology*; Wiley & Sons, Inc: New York, 2005. (b) Kissin, Y. V. In *Kirk-Othmer Encyclopedia of Chemical Technology*; Wiley & Sons, Inc: New York, 2005.

(2) Dixon, J. T.; Green, M. J.; Hess, F. M.; Morgan, D. H. *J. Organomet. Chem.* **2004**, *689*, 3641–3668.

(3) Wass, D. F. *Dalton Trans.* **2007**, *816*, 819.

10.1021/om800326r CCC: $40.75
Publication on Web 09/04/2008

Table 1. Investigated Ligands With Their Experimental Product Composition[a]

catalyst	C6, g (wt %)	C10, g (wt %)	PE, g (wt %)	productivity[b]
1[c]	20.9 (83)	3.5 (14)	0.5 (1.8)	2787
2[c]	2.7 (42)	0.6 (9)	2.2 (34)	NA
3[c]	2.1 (36)	0.4 (7)	2.6 (44)	NA
4[c]	24.4 (87)	2.9 (10)	0.6 (2.0)	650
5[c]	0.5 (17)	0.1 (4)	2.4 (76)	66
6[d]	0.038 (90)	NA	0.004	25
7[c]	7.9 (93)	0.5 (5)	0.1 (1.3)	1053

[a] Catalytic ethene conversion with the catalyst/MAO systems (toluene solvent, 5 bar of ethene, 30 °C, 15 mmol of Ti, Al:Ti 1000, 30 min run time). [b] In kg C_6 product per mole Ti per h. [c] Data taken from ref 6b. [d] Data taken from Wu, T.; Qian, Y.; Huang, J. *J. Mol. Catal. A: Chem.* **2004**, *214*, 227−229. $T = 80$ °C and 3 μmol of catalyst. Note that at $T = 30$ °C there is hardly any activity.

corresponds to the co-oligomerization of two ethylene molecules with one molecule of 1-hexene (Table 1, catalyst **1**).

To improve the understanding and to explain this high selectivity, several computational studies have been performed,[7] and essentially all confirmed the proposed mechanism of Deckers and co-workers (see Scheme 1). Additionally, these theoretical results provided a better understanding of the catalyst's activation[7c] and the different mechanisms that operate during ring-opening reactions.

The enhanced understanding of the mechanism for the trimerization reactions themselves has also provided insights into their possible side-reactions yielding 1-butene or larger (than 1-hexene) α-olefins for example.[7b]

Tobisch and Ziegler have extended the comprehension and predicted the reaction outcome of this type of trimerization

Scheme 1

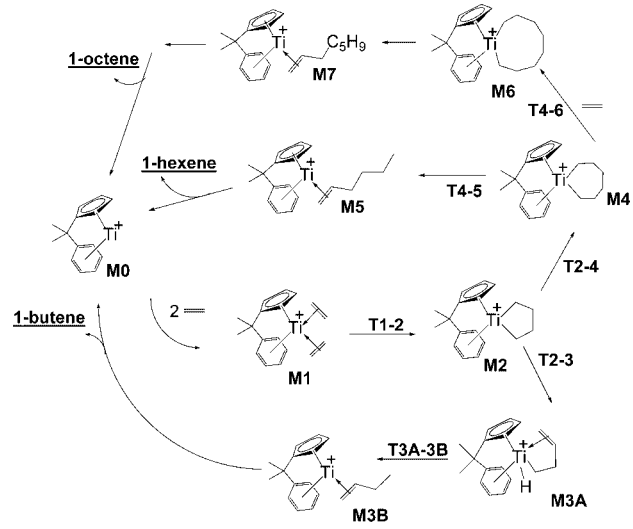

reactions in several theoretical studies in which first the titanium cation has been replaced by the heavier metals ions of group IV, zirconium and hafnium,[8] second, effects of electron-donating/withdrawing groups in the aryl were investigated,[9] and, third, the cyclopentadienyl moiety was interchanged for boratabenzenes,[10] preserving the heavier Zr and Hf elements in the two latter studies.

Here, we report a DFT computational approach investigating the changes in the selectivity and activity of the trimerization or oligomerization reaction as a function of variations in the nature of the R-group and in the bridge X that connects the cyclopentadienyl and the R-group in the Ti complexes that have been studied. It is our objective to provide for the experimental chemist a structure/selectivity relationship based on a relevant chemical descriptor that can be used to predict whether the titanium-cyclopentadienyl catalyst will more likely produce simple olefins, such as 1-hexene, or whether multiple insertion reactions of ethylene are to be expected. It is important to underline that we thus (hypothetically) presume in this study that, independent of the nature of R and X, all catalysts can be activated in such a way that the active species enter the metallacyclic mechanistic pathway as described in Scheme 1 for catalyst **1**.

Charts 2 and 3 display in total 15 catalytic systems that have been studied, presented in their supposed activated bare form, since we presume in this theoretical study that all precatalysts can be activated by MAO to yield the highly reactive bare catalysts that enter the catalytic cycle as depicted in Scheme 1. The first seven catalytic systems used to construct the structure/selectivity relationship are displayed in Chart 2, and the corresponding experimental data are presented in Table 1. This table shows that both the type of ligand (R) and the nature of the functional bridging group (X) can dramatically alter the overall outcome of the reaction. For example, while changed product ratios are observed upon modification of the nature of the bridging functional group (compare catalysts **1** with **2** and **3**), upon changing the phenyl (catalyst **1**) by a methyl group (catalyst **5**), the catalyst principally yields polyethylene (PE). Although the PE produced by the latter catalyst is likely the result of a polymerization that has not followed a metallacyclic

(4) (a) Agapie, T.; Schofer, S. J.; Labinger, J. A.; Bercaw, J. E. *J. Am. Chem. Soc.* **2004**, *126*, 1304–1305. (b) Janse van Rensburg, W.; Grove, C.; Steynberg, J. P.; Stark, K. B.; Huyser, J. J.; Steynberg, P. J. *Organometallics* **2004**, *23*, 1207–1222. (c) McGuinness, D. S.; Wasserscheid, P.; Morgan, D. H.; Dixon, J. T. *Organometallics* **2005**, *24*, 552–556. (d) McGuinness, D. S.; Brown, D. B.; Tooze, R. P.; Hess, F. M.; Dixon, J. T.; Slawin, A. M. Z. *Organometallics* **2006**, *25*, 3614–3619. (e) Schofer, S. J.; Day, M. W.; Henling, L. M.; Labinger, J. A.; Bercaw, J. E. *Organometallics* **2006**, *25*, 2743–2749. (f) Temple, C.; Jabri, A.; Crewdson, P.; Gambarotta, S.; Korobkov, I.; Duchateau, R. *Angew. Chem., Int. Ed.* **2006**, *45*, 7050–7053. (g) Janse van Rensburg, W.; van den Berg, J.-A.; Steynberg, P. J. *Organometallics* **2007**, *26*, 1000–1013. (i) Nenu, C. N.; Bodart, P.; Weckhuysen, B. M. *J. Mol. Catal. A: Chem.* **2007**, *269*, 5–11. (j) McGuinness, D. S.; Rucklidge, A. J.; Tooze, R. P.; Slawin, A. M. Z. *Organometallics* **2007**, *26*, 2561–2569. (k) Bollmann, A.; Blann, K.; Dixon, J. T.; Hess, F. M.; Killian, E.; Maumela, H.; McGuinness, D. S.; Morgan, D. H.; Neveling, A.; Otto, S.; Overett, M.; Slawin, A. M. Z.; Wasserscheid, P.; Kuhlmann, S. *J. Am. Chem. Soc.* **2004**, *126*, 14712–14713. (l) Elowe, P. R.; McCann, C.; Pringle, P. G.; Spitzmesser, S. K.; Bercaw, J. E. *Organometallics* **2006**, *25*, 5255–5260. (m) Kuhlmann, S.; Blann, K.; Bollmann, A.; Dixon, J. T.; Killian, E.; Maumela, M. C.; Maumela, H.; Morgan, D. H.; Pretorius, M.; Taccardi, N.; Wasserscheid, P. *J. Catal.* **2007**, *245*, 279–284. (n) McGuinness, D. S.; Overett, M.; Tooze, R. P.; Blann, K.; Dixon, J. T.; Slawin, A. M. Z. *Organometallics* **2007**, *26*, 1108–1111. (o) Rucklidge, A. J.; McGuinness, D. S.; Tooze, R. P.; Slawin, A. M. Z.; Pelletier, J. D. A.; Hanton, M. J.; Webb, P. B. *Organometallics* **2007**, *26*, 2782–2787. (p) Agapie, T.; Labinger, J. A.; Bercaw, J. E. *J. Am. Chem. Soc.* **2007**, *129*, 14281–14295.

(5) (a) Andes, C.; Harkins, S. B.; Murtuza, S.; Oyler, K.; Sen, A. *J. Am. Chem. Soc.* **2001**, *123*, 7423–7424. (b) Yu, Z. X.; Houk, K. N. *Angew. Chem., Int. Ed.* **2003**, *42*, 808–811.

(6) (a) Deckers, P. J. W.; Hessen, B. *Organometallics* **2002**, *21*, 5564–5575. (b) Deckers, P. J. W.; Hessen, B.; Teuben, J. H. *Organometallics* **2002**, *21*, 5122–5135. (c) Deckers, P. J. W.; Patrick, J. W. Non Flory-Schulz Ethene Oligomerization with Titanium-based Catalysts. Ph.D. Thesis, 2002. (d) Deckers, P. J. W.; Hessen, B.; Teuben, J. H. *Angew. Chem., Int. Ed.* **2001**, *40*, 2516–2519. (e) Hessen, B. *J. Mol. Catal. A: Chem.* **2004**, *213*, 129–135. (f) Wang, C.; Huang, J. L. *Chin. J. Chem.* **2006**, *24*, 1397–1401.

(7) (a) Blok, A. N. J.; Budzelaar, P. H. M.; Gal, A. W. *Organometallics* **2003**, *22*, 2564–2570. (b) De Bruin, T. J. M.; Magna, L.; Raybaud, P.; Toulhoat, H. *Organometallics* **2003**, *22*, 3404–3413. (c) Tobisch, S.; Ziegler, T. *Organometallics* **2003**, *22*, 5392–5405.

(8) Tobisch, S.; Ziegler, T. *J. Am. Chem. Soc.* **2004**, *126*, 9059–9071.

(9) Tobisch, S.; Ziegler, T. *Organometallics* **2004**, *23*, 4077–4088.

(10) Tobisch, S.; Ziegler, T. *Organometallics* **2005**, *24*, 256–265.

Chart 2

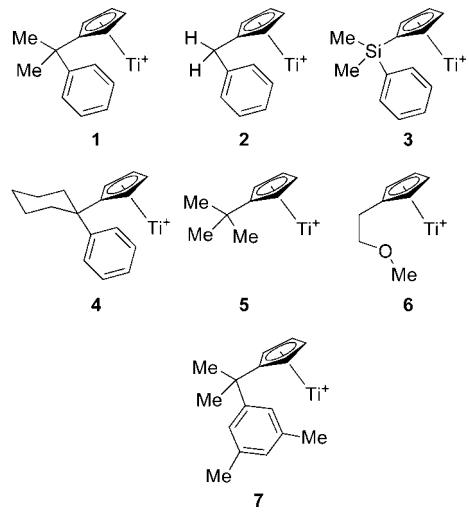

Chart 3

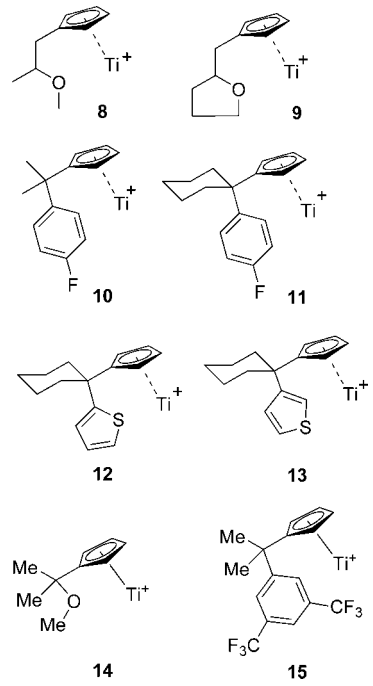

mechanistic pathway,[11] but a degenerated mechanistic pathway as proposed by Cossee−Arlman,[12] we have considered this catalyst as the others for comparison reasons. However, more generally, the formation of polyethylene following a metallacyclic pathway should not be excluded, considering the experimental results of Gibson et al. with a chromium-based catalyst.[13]

Next, the obtained structure/selectivity relationship is applied to a set of ligands for which experimental data are available but were not used in the "training set". Finally, we will apply the found relationship to some catalysts for which at this moment experimental data are not available, and the product composition will thus be predicted.

In this computational study, we thus attempt to rationalize the experimentally observed differences in product compositions. In order to do so, we compare the geometrical structures and

(11) Briggs, J. R. *Chem. Commun.* **1989**, *674*, 675.
(12) Arlman, E. J.; Cossee, P. *J. Catal.* **1964**, *3*, 99–104.
(13) Tomov, A. K.; Chirinos, J. J.; Jones, D. J.; Long, R. J.; Gibson, V. C. *J. Am. Chem. Soc.* **2005**, *127*, 10166–10167.

Scheme 2

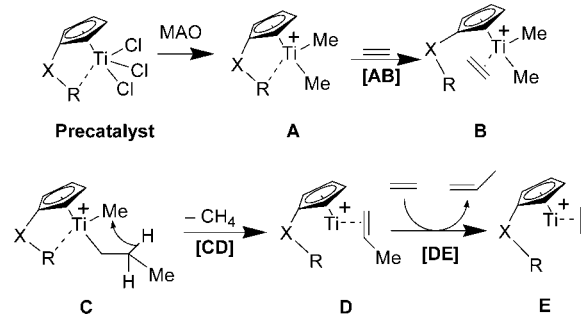

their corresponding energies for species that were previously identified using density functional theory, to determine the activity and selectivity of the trimerization of ethylene.

It appeared from previous theoretical studies that the uptake and insertion reaction of the third ethylene molecule is the rate-determining step. Furthermore, the selectivity is determined by the difference in energy between two energy barriers: (i) the one to pass the barrier for the ring-opening reaction of the seven-membered metallacycle (**T4-5**) and (ii) that to pass the barrier for the uptake and insertion of the fourth ethylene molecule (**T4-6**), cf. Scheme 1.[7]

In the present study, we presume that all the presented catalysts can be activated to give the active species **M1**. Tobisch and Ziegler have shown a plausible pathway for the formation of such active species, from the titanium dimethyl cation, which in turn was formed from the titanium trichloride precatalyst after activation with the cocatalyst MAO (Scheme 2).

In the following, we first outline the details of the calculations, discuss the geometries of the optimized structures and their energetics to rationalize the observed experimental outcome, and derive a structure/selectivity relationship. The last section is dedicated to the conclusions.

2. Theoretical Methods

All geometry optimization calculations have essentially been performed with the Jaguar software package[14] and occasionally with Gaussian 03.[15] The B3LYP functional has been applied in the form as implemented in both programs, i.e., with the VWN functional III for the local correlation,[16] in combination with the following basis set. The titanium element was described with the pseudopotential LanL2DZ,[17] in which an effective core potential was used to describe the inner first 10 electrons. For the elements carbon, oxygen, silicon, and hydrogen the 6-31G(d,p) all-electron basis set was used. This double-ζ basis set was extended with a set of diffuse functions (6-31+G(d,p)) in order to take better into account the

(14) *Jaguar*, Version 5.5; Schrödinger Inc.: LLC, Portland, OR, 2003.
(15) Frisch, M. J.; Trucks, G. W.; Schlegel, H. B.; Scuseria, G. E.; Robb, M. A.; Cheeseman, J. R.; Montgomery, J. A., Jr.; Vreven, T.; Kudin, K. N. ; Burant, J. C.; Millam, J. M.; Iyengar, S. S.; Tomasi, J.; Barone, V.; Mennucci, B.; Cossi, M.; Scalmani, G.; Rega, N.; Petersson, G. A.; Nakatsuji, H.; Hada, M.; Ehara, M.; Toyota, K.; Fukuda, R.; Hasegawa, J.; Ishida, M.; Nakajima, T.; Honda, Y. ; Kitao, O.; Nakai, H.; Klene, M.; Li, X.; Knox, J. E.; Hratchian, H. P.; Cross, J. B.; Adamo, C.; Jaramillo, J.; Gomperts, R.; Stratmann, R. E.; Yazyev, O.; Austin, A. J.; Cammi, R.; Pomelli, C.; Ochterski, J. W.; Ayala, P. Y.; Morokuma, K.; Voth, G. A.; Salvador, P.; Dannenberg, J. J.; Zakrzewski, V. G.; Dapprich, S.; Daniels, A. D.; Strain, M. C.; Farkas, O.; Malick, D. K.; Rabuck, A. D.; Raghavachari, K.; Foresman, J. B.; Ortiz, J. V.; Cui, Q.; Baboul, A. G.; Clifford, S.; Cioslowski, J.; Stefanov, B. B.; Liu, G.; Liashenko, A.; Piskorz, P.; Komaromi, I.; Martin, R. L.; Fox, D. J.; Keith, T.; Al-Laham, M. A.; Peng, C. Y.; Nanayakkara, A.; Challacombe, M.; Gill, P. M. W.; Johnson, B.; Chen, W.; Wong, M. W.; Gonzalez, C.; Pople, J. A. *Gaussian 03*, Revision B.05; Gaussian Inc.: Pittsburgh, PA, 2003.
(16) Becke, A. D. *J. Chem. Phys.* **1993**, *98*, 5648–5652.
(17) Hay, P. J.; Wadt, W. R. *J. Chem. Phys.* **1985**, *82*, 299–310.

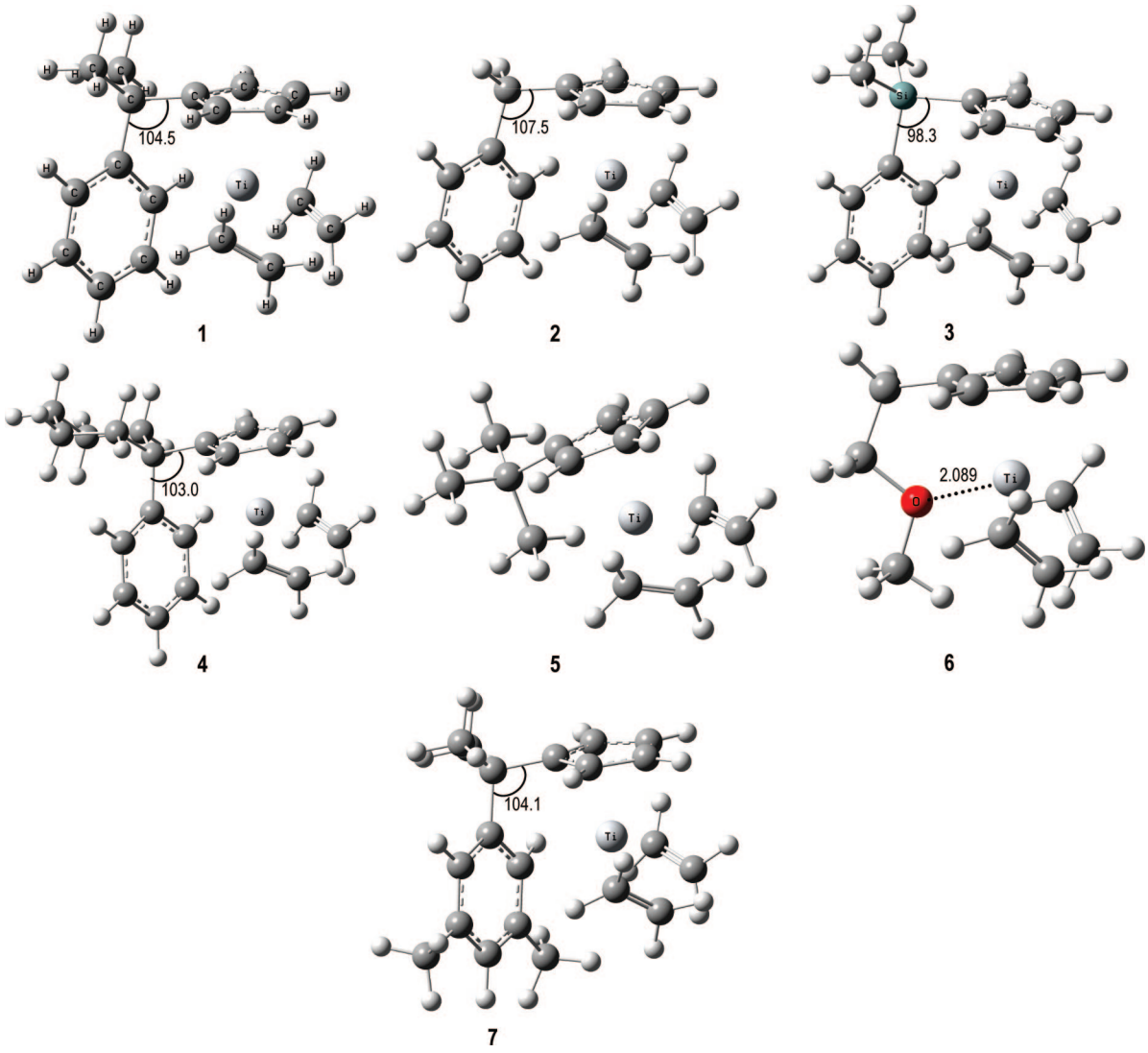

Figure 1. Geometrical features of the **M1** species for catalysts **1**−**7**.

electron-withdrawing properties in the case of the fluorine element. The pseudospectral method was used for the geometry optimizations realized with the Jaguar program. It has previously been shown that this method influences neither the final geometry nor the final energy.[7b] No geometrical constraints were applied, except for the product containing the cyclopentadienyl moiety that is formed in the isodesmic reactions, eq 1. For this product, only the atoms in blue, i.e., the CH_3 (or SiH_3) group, were relaxed, whereas all other atoms have been frozen. All species were expected to be in the singlet electronic ground state, as was verified for the system R = phenyl.[7b] Practically all starting geometries were optimized with the spin-restricted formalism, and the corresponding stationary points on potential energy surface were subjected to a frequency analysis.[18] The normal modes were calculated with the default harmonic oscillator approach; neither corrections for hindered rotations nor anharmonicities were taken into account. It was verified that each stationary point had the desired character (minimum or transitions state). Furthermore, with the use of partition functions, the internal energy, and entropic contributions to the Gibbs free energy could be calculated. All reported Gibbs free energy values were calculated at $T = 298$ K and $P = 1$ atm.

(18) It was found that for the optimization of some transition states the number of steps could be reduced if the unrestricted spin formalism was applied. This was however only valid for old versions of Jaguar, i.e., version 5.5 or older. For the more recent version of Jaguar this particularity was not observed.

3. Results and Discussion

3.1. Geometries. The optimized geometries in which two ethylene molecules are coordinated to the Ti(II) cation, species **M1**, for catalysts **1**−**7** are presented in Figure 1. Significant changes in the optimized geometries can be observed: they result from fairly minor variations in the topology of the catalyst. For example, it can be seen that upon interchanging the carbon in **1** by a silicon atom, as in **3**, the bond angle of the bridge connecting the cyclopentadienyl group and the R-group is significantly reduced from 104.5° to 98.3°. In other words, the silicon atom induces a tighter bonding of the phenyl group to the titanium cation than the carbon atom, as concluded from the Ti−C(Aryl) bond length, which is slightly longer in **1** as compared to **3**.

The electron-donating effects of the two methyl groups on the phenyl ligand induce a stronger interaction of the phenyl moiety toward the metal ion, as can be seen by a small decrease in the shortest Ti−C(Aryl) bond length: 2.397 Å in **7** and 2.401 Å in **1**.

The catalysts containing an ether functionality (**6**) show a somewhat different structure. The oxygen atom strongly interacts with the titanium cation (bond length is 2.089 Å), which is significantly shorter than the shortest Ti−C(Aryl) observed for **7**.

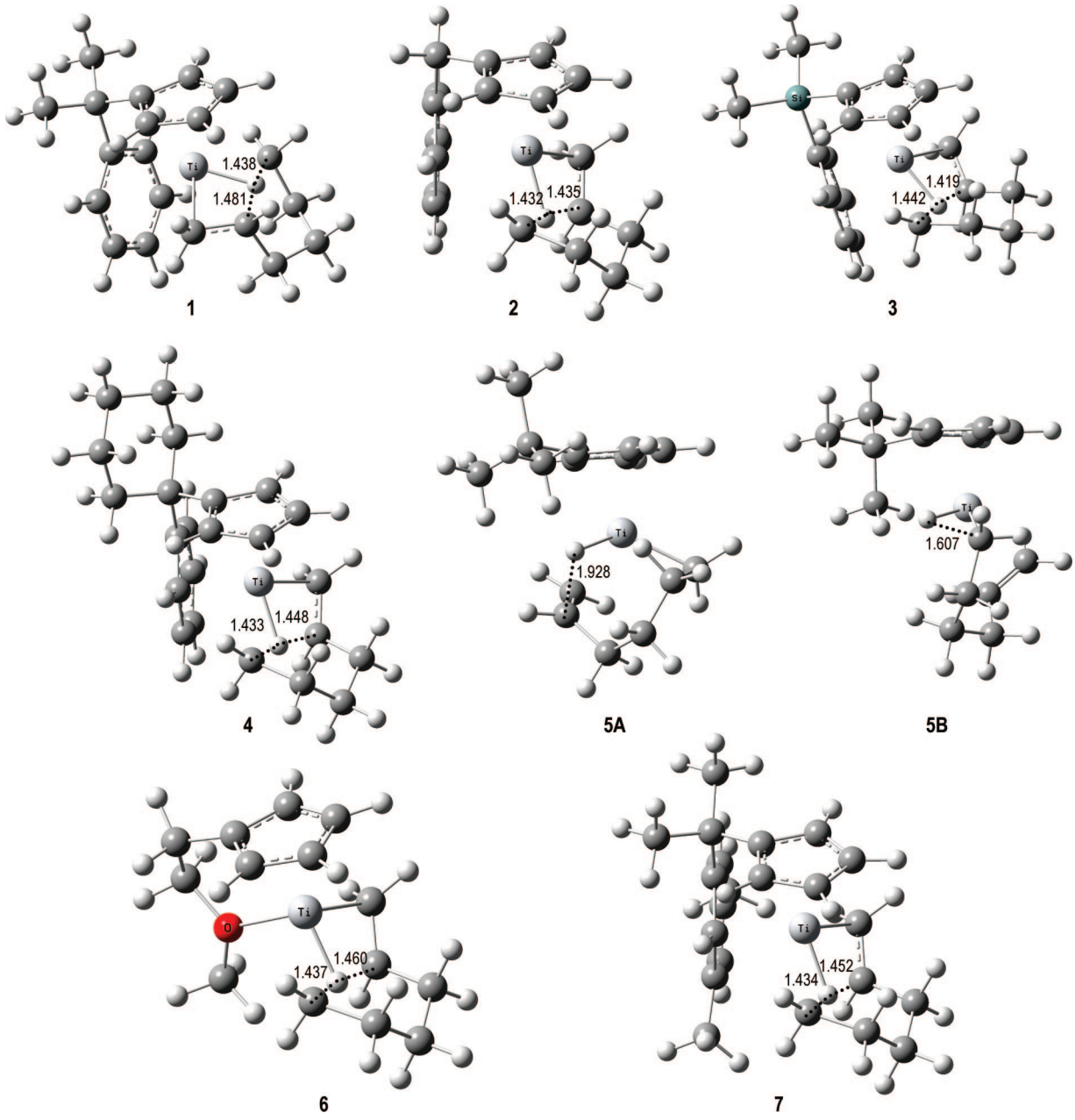

Figure 2. Geometrical features of the **T4-5** transition state structures for catalysts **1**−**7**.

The transition state **T4-5**, which characterizes the ring-opening reaction via β-hydrogen transfer, and the transition state **T4-6**, which corresponds to the uptake and insertion of the fourth ethylene molecule, are presented for the catalysts **1** to **7** in Figures 2 and 3, respectively. When it is assumed that catalyst **5** can enter the metallacyclic pathway, important differences are observed as compared to the other catalysts in the sense that the hydrogen transfer is a two-step reaction, in which the hydrogen is first transferred to the metal ion and then to α-C carbon atom of the formed C_6H_{12} olefin. For all other catalysts, this transfer occurs via a concerted step, where the hydride is directly transferred from the 2 (or β) position to the 6 position, although of course this migration is assisted by the Ti cation.

Concerning the geometrical features of the transition states for the insertion of the fourth ethylene molecule, only minor differences for the different catalysts can be observed. The carbon−carbon bond to be formed varies in the transition states from 2.194 Å for catalyst **6** to 2.271 Å for catalyst **5**.

No general trend could be observed based only upon the geometrical features. Comparison of geometrical features is moreover complicated due to the different nature of the ligand: substituted phenyls versus ether type ligands.

However, the variation in the interaction energy between ligand and metal ion during the catalytic cycle expressed in the form of energy for each ligand would make the comparisons more universal. In the next paragraph it is presented how this energy is calculated and how it relates to the product formation experimentally observed.

3.2. Energetics and Product Formation. Since Deckers et al.[6b] and Tobisch and Ziegler[7c,9] already showed the importance of the lability of the pendent ligand, it is rational to quantify this property by calculating the energy required to dissociate the pendent ligand from the metal ion.

Different approaches to calculate this dissociation energy can be proposed, for example, by rotation of the corresponding dihedral angle. However, for the catalysts with an ether

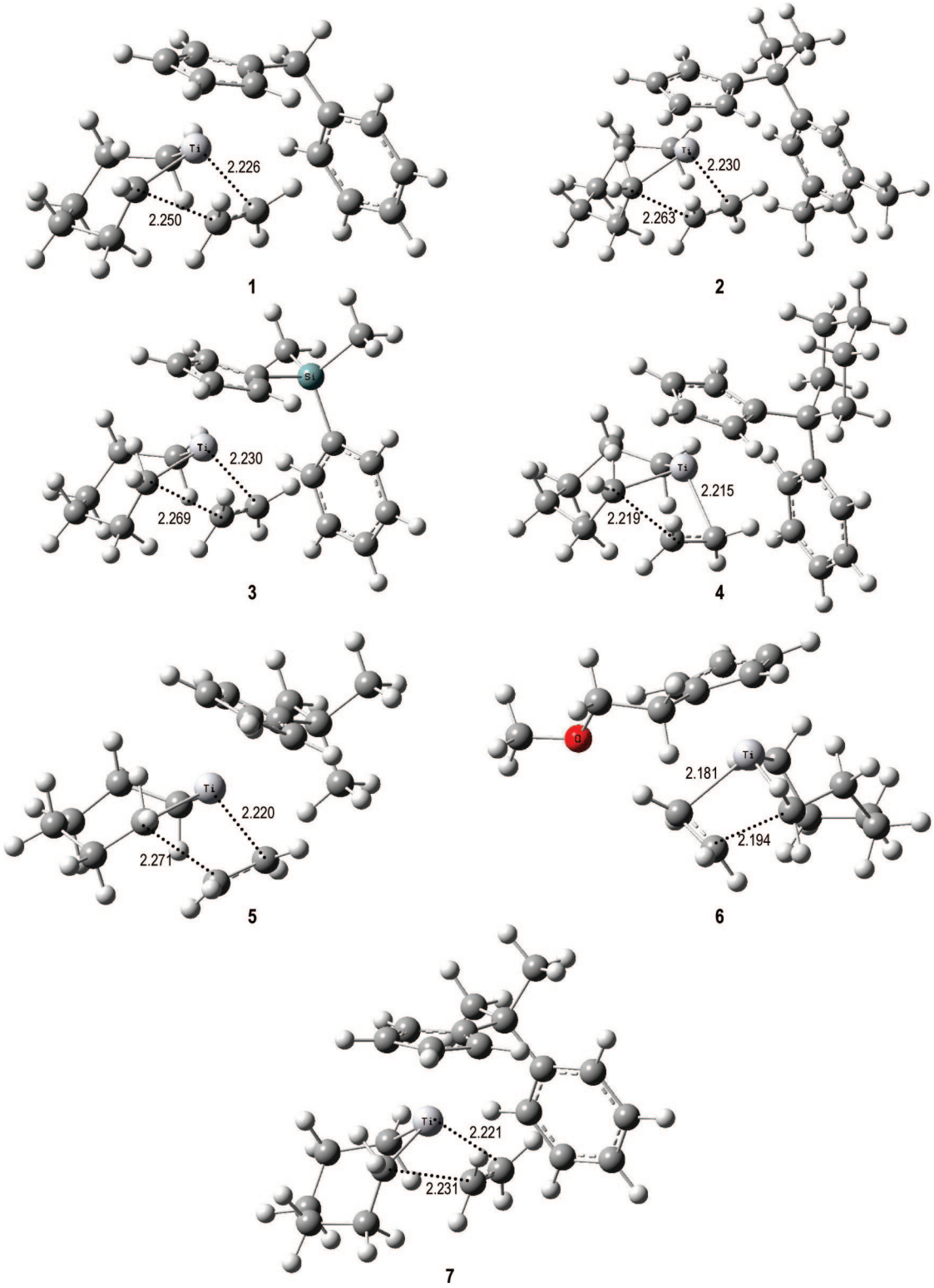

Figure 3. Geometrical features of the **T4-6** transition state structures for catalysts **1**−**7**.

functionality, such a constrained geometry optimization fails in the sense that the forces left on atoms remain too large, with respect to the general convergence criteria. Moreover, for catalyst **5**, no dihedral angle can be chosen in which there is no interaction of the methyl group with the metal ion.

These kinds of problems can be avoided by the use of an isodesmic reaction, in which the same number and type of chemical bonds can be found on the left- and right-hand side of the equation. The isodesmic reaction used in this study is presented in eq 1 and has been chosen in such a way that it evaluates the interaction of the ligand R with the Ti cation. It should be noticed that in the case of catalyst **3**, SiH_4 is formed instead of methane and the cyclopentadienyl is substituted with a SiH_3 group.

Table 2 summarizes the calculated dissociation energy (E_{diss}) using the changes in electronic energy, i.e., without thermodynamic corrections, for species **M1** and the transition states **T4-5** and **T4-6**.

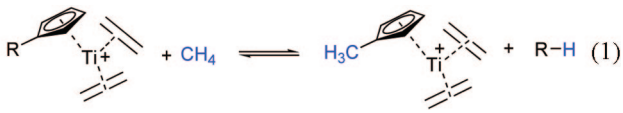

(1)

The interaction between the ligand and the titanium cation ranges from 2.2 to 37.0 kcal/mol for the **M1** species. As expected from chemical intuition, the catalyst containing a methyl group (**5**) has only a very weak interaction with the metal ion, principally resulting from the CH_3 hydrogen−titanium interaction. It can also be seen that the aryl without electron-donating groups (catalyst **1**) has a smaller interaction than catalyst **7**, containing two methyl groups: 15.2 kcal/mol versus 17.7 kcal/mol. The substitution of a carbon atom for a silicon atom significantly increases the dissociation energy from 15.2 to 24.3. This phenomenon had already been seen previously when the geometrical features of catalyst **3** were discussed. The strongest interactions are calculated for the catalyst **6**, which contains an ether−oxygen interaction with the metal ion.

More precisely, the dissociation energy, calculated via a virtual isodesmic reaction, is one way to account for two predominant effects controlling the interaction between the pendent group and the Ti cation: the electronic affinity of the ligand for the Ti centers and the structural flexibility of the organometallic complex. The natural population analysis reveals that the charge on the Ti center can account for the values of dissociation energy. In coherence with the structural flexibility, we observe a charge redistribution around the Ti center, resulting in a near constant natural charge on Ti: 0.866*e* for catalyst **1**; 0.972*e* for catalyst **5**; and 0.978*e* for catalyst **6**. It appears from isoelectron density surfaces of the **M1** structures that the electron density in catalyst **5** is located more on the ethylene and cyclopentadienyl carbon atoms, whereas in catalyst **6** it is on the oxygen atom of the ether group.[19]

When we now compare the calculated dissociation energies for the two transition states for ring opening toward 1-hexene and for the insertion of the fourth ethylene molecule, the following tendency is observed. For all ligands (except the methyl group), the R-group is more strongly coordinated to the metal in the transition state for the ring opening than in its corresponding **M1** structure. Conversely, the dissociation is smaller in the transition state for the insertion reaction of the ethylene molecule (**T5-6** structures) than in the corresponding **M1** geometry. The small negative dissociation energies could be the result of minor repulsive interactions in the case of transition state structure with respect to corresponding reactants in eq 1.

From these observations, it can be concluded that each R-group behaves as a ligand that coordinates more strongly or weakly to the metal ion according to its nucleophilic character. The only exception is the methyl group, which behaves as a completely labile R-group along the whole pathway.

It is now interesting to see how these dissociation energies relate to the energy barriers of **T4-5** and **T4-6** with respect to **M4**. First, we analyze these barriers reported in Table 3. It can be seen that the energy barrier required for the ring opening is nearly constant. In other words, the nature of the ligand has only a minor effect on the ring-opening reactions. In contrast, the insertion reaction of the fourth ethylene molecule is far more sensitive. In this case, the barriers vary from 12.3 for the catalyst with the methyl group to 29.7 kcal/mol in the case of catalyst **6**, which contains an ether functionality.

Taking into account the data of Tables 1 and 3, it becomes clear that ring-opening reactions are favored by a strong interaction of the ligand with respect to the insertion reaction that is more favored by more labile R-groups. For example, in catalyst **5**, the methyl group has only a weak interaction with the titanium ion, has the highest barrier for the ring-opening reaction, whereas for the insertion reaction it shows the lowest barrier. From Table 3, it is seen that nearly all ligands have the same energy barrier for ring-opening, around 20 kcal/mol, except catalyst **5**, for which the barrier is calculated to be 23.3 kcal/mol. This is also the only catalyst in which the dissociation energy has diminished in **T4-5** (1.5 kcal/mol) with respect to **M1** (2.2 kcal/mol). Apart from catalyst **5**, all other catalysts have rather similar activation energies, suggesting that the nature of the ligand does not influence too much the energy barrier for ring opening. This relative indifference might be the result of the fact that the β-hydrogen transfer does not require the dissociation of the ligand. In fact, it is seen from the dissociation energies that the ligands interact slightly stronger with the titanium cation in the **T4-5** species than in **M1**. This slightly amplified interaction is likely due to the reduction of the metal ion from oxidation state 4 to 2, requiring two electrons.

The situation is quite different for the uptake and insertion reaction of the fourth ethylene molecule. In this case, the ligand needs to dissociate from the metal in order to diminish the steric hindrance for the incoming ethylene. This is supported by the data presented in Table 2 (column 3), where it is shown that for all catalysts the ligand in **T4-6** is (nearly) dissociated, as can be seen by the small dissociation energies. The catalyst with the stronger coordinating ether functionality (catalyst **6**) will therefore exhibit a high energy barrier for insertion (29.7 kcal/mol), whereas the labile methyl group (catalyst **5**) has a small barrier (12.3 kcal/mol). It therefore becomes clear that more labile ligands dissociate easier and thus will favor multiple ethylene insertions. The importance of the nature of the ligand on this barrier was also found by Tobisch and Ziegler for analogous zirconium complexes.[9]

In the following part the calculated energy barriers will be compared and related to the available experimental data.

For catalysts **1**, **4**, **6**, and **7**, the lowest barrier is calculated for the ring-opening reaction of the seven-membered ring,

Table 2. Dissociation Energies (kcal·mol^{-1}) Calculated According to Eq 1

ligand	M1	T4-5	T4-6
1	15.2	21.7	−2.7
2	16.4	20.9	0.5
3	24.3	27.1	7.4
4	22.9	29.1	6.6
5	2.2	1.5	−2.0
6	37.0	40.9	5.6
7	17.7	23.2	−1.9

Table 3. Energy Barriers ($\Delta G^{\ddagger}$(298 K)) for the Transitions M4 → T4-5 and M4 → T4-6 (in kcal·mol^{-1})

catalyst	M4 → T4-5	M4 → T4-6
1	18.4	24.3
2	20.0	21.1
3	19.9	19.7
4	19.4	25.2
5	23.3	12.3
6	18.2	29.7
7	20.8	25.5

(19) The isoelectron density surfaces for catalysts **1**, **5**, and **6** for the **M1** structure are available in the Supporting Information.

(20) Since ring-opening reactions, either of a five- or seven-membered metallacycle, are favored by nonlabile ligands, the ring opening of the five-membered ring to yield 1-butene is a plausible side-reaction. It has however been verified that for catalyst **6**, which experiences the largest coordination energy, the energy barrier to yield 1-butene is larger than the barrier to insert the third ethylene molecule.

leading to 1-hexene as the major product formed, which is in accordance with experiments. However, for catalyst **5**, with its noncoordinating methyl group, the lower barrier is computed for the insertion reaction, suggesting that 1-hexene is the minor product. Therefore, even in the case where catalyst **5** follows a metallacyclic mechanistic pathway, longer oligomers than hexene-1 are expected. Alternatively, the produced polyethylene by catalyst **5** is likely the result of multiple insertion reactions of ethylene following a Cossee−Arlman mechanism during the process of activation (species **B** and **C** in Scheme 2).

For catalysts **2** and **3** the calculated barriers for the two competing reactions are nearly equal, predicting a mixture of 1-hexene and PE in practically equal amount. This is once more experimentally confirmed. Generally, on the basis of the comparison of the barrier heights of the two competing reactions, an excellent accord is found with the experimental data.

It is however far more difficult to predict the activity. In earlier studies it has been pointed out that the uptake and insertion of the third ethylene molecule is the rate-determining step for catalyst **1**. If one now assumes that the reaction barrier of the uptake and insertion reaction of the fourth ethylene molecule is proportional to that of the third ethylene molecule, one of the highest activities would be obtained for catalyst **1**, followed by catalyst **4** and finally **7**. Indeed for **1** the most important activity is observed, but **7** is experimentally more active than **4**. Catalysts **2** and **3** should be more productive than **1**, yet the contrary is experimentally observed. Even more dramatic is the case for catalyst **5**, which has the lowest energy of all catalysts (12.3 kcal/mol) for the fourth ethylene molecule uptake and insertion reaction, yet it is nearly inactive. This therefore suggests that the PE formed by catalyst **5** is not the result of (very) large metallacycles, but is more likely formed via the Cossee−Arlman mechanism.

Predictions for New Ligands. Although the reaction barriers for the ring-opening reaction of the seven-membered ring and the barrier for the uptake and insertion of the fourth ethylene molecule describe correctly the reaction selectivity, the calculation of such barriers is rather long and cumbersome. It would be of high interest if one could easily anticipate for a given catalytic system whether the ligand will lead to 1-hexene or, in contrast, to multiple insertions.

It would therefore be a great help if a simple chemical descriptor could be computed that indicates that above or below a certain change in reaction energy the catalytic system favors 1-hexene or PE.

In Figure 4 the Gibbs free energy reaction barriers for the two steps determining the reaction selectivities have been plotted against the dissociation energy of the pendent R-group. As seen already, the energy barrier for the ring-opening reaction is lowered upon increased dissociation energy of the ligand, although this dependency is rather small. This is translated in Figure 4 by a graph in which the Gibbs free energy barrier for ring opening is expressed in terms of the dissociation energy with the following linear equation possessing a negative slope: $\Delta G^{\ddagger}_{T4-5} = -0.1247E_{diss} + 22.456$. On the other hand, the Gibbs free energy barrier is lowered for more labile ligands and thus has a positive slope: $\Delta G^{\ddagger}_{T4-6} = 0.429E_{diss} + 14.208$. The larger slope corresponds to a higher sensitivity of the energy barrier height with respect to the dissociation energy.

The two graphs cross each other at a dissociation energy near 15 kcal/mol. At this point, the ratio of reaction rate for ring opening and the rate for ethylene insertion equals zero. For catalytic systems in which the dissociation energy is less than 15 kcal/mol, multiple uptake and insertion reactions of ethylene

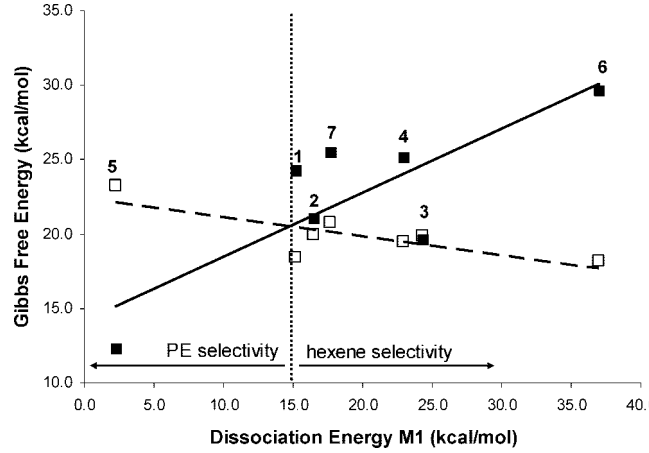

Figure 4. Correlation between the free energy barriers for ring opening, **T4-5** (open squares), and ethylene insertion, **T4-6** (filled squares), and the dissociation energy of the hemilabile ligand in **M1** for catalysts **1**−**7**.

Table 4. Investigated Ligands with Their Experimental Product Composition

catalyst	ΔE_{diss} (kcal/mol)	C6 (g (wt %))	PE (g)	productivity[b]
8[cd]	41.5	0.080 (>95)	trace	57
9[c]	43.5	0.042 (93)	0.004	25
10[e]	15.7	0.0461 (85)	0.008	61.5
11[e]	19.3	0.3747 (97)	0.0104	499.6
12[f]	17.4	0.117 (84)	0.017	156
13[f]	18.7	0.014 (12)	0.094	19
14	31.0	NA	NA	NA
15	8.3	NA	NA	NA

[a] Catalytic ethene conversion with the catalyst/MAO systems (toluene solvent, 5 bar of ethene, 30 °C, 1.5 μmol of Ti; Al:Ti = 1000; 30 min run time, unless stated otherwise). [b] In kg C_6 product per mole Ti per h. [c] Data taken from Wu, T.; Qian, Y.; Huang, J. *J. Mol. Catal. A: Chem.* **2004**, *214*, 227−229. Concentration: 3.0 μmol of catalyst. [d] T = 80 °C. [e] Data taken from Wang, C.; Huang, J. L. *Chin. J. Chem.* **2006**, *24*, 1397−14. [f] Data taken from Huang, J.; Wu, T.; Qian, Y. *Chem. Commun.* **2003**, 2816−2817.

are to be expected, whereas for those systems where this dissociation energy is greater, 1-hexene will likely be the major product.[20]

This simple chemical descriptor provides a rather good estimation for catalysts **1**−**7**, although for catalysts **2** and **3**, which have dissociation energies larger than 15 kcal/mol, also a substantial quantity of PE is detected. Again, part of the formed PE might be the result of a polymerization reaction following the Cossee−Arlman mechanism.

To test further the viability of this descriptor, the dissociation energy, calculated with the use of the isodesmic reaction eq 1, of the **M1** species has been calculated for six additional catalytic systems (**8**−**13**), for which experimental data are also available. The activated bare catalysts are presented in Chart 3 and their dissociation energy together with their experimentally selectivity in Table 4.

All ligands in **8**−**13** have a dissociation energy greater than 15 kcal/mol, suggesting that 1-hexene should be the major product. The calculated predictions are in accordance with the experimental results, except for catalyst **13**, for which PE is the major product. This disagreement could not be rationalized. The model was also applied to two catalysts (**14** and **15**) for which, to best of our knowledge, no experimental data are available. According to the calculated dissociation energies and the relation derived in Figure 4, catalyst **14** should predominantly yield 1-hexene, whereas for catalyst **15**, which has a

dissociation energy smaller than 15 kcal/mol, multiple insertion reactions are to be expected.

4. Concluding Remarks

The influence of the role of the hemilabile ligand in titanium-based complexes as developed by Teuben et al. to selectively produce 1-hexene resulting from the trimerization reaction of ethylene has been explored with the use of density functional theory (B3LYP functional). The already identified competing reaction pathways, i.e., the ring opening of the seven-membered ring and uptake and insertion of the fourth ethylene molecule, have been explored for in total 15 catalytic systems. These energy barriers have been related with the simple chemical descriptor that represents the dissociation energy that is required to dissociate the R-group from the titanium cation in the **M1** structure. It is found that the ring-opening reaction is far less sensitive to the dissociation energy of the ligands than for the uptake and insertion reaction. The nature of the pendent R-group therefore plays a major role in the insertion reaction. From a prediction model derived from seven catalysts, it appears that for catalytic systems with ligands having dissociation energies less than 15 kcal/mol, multiple insertion reactions are likely to occur, whereas for ligands with dissociation energies larger than 15 kcal/mol, ring opening occurs, leading to 1-hexene production. This chemical descriptor has been applied to six other catalysts (**8**−**13**). Only for catalyst **13** a disagreement is found between our model and the experimental data. For catalysts **14** and **15**, where no experimental data are available, the model predicts 1-hexene and polyethylene, respectively, the latter resulting from multiple insertion reactions, as the major products.

Acknowledgment. The authors thank Drs. H. Olivier-Bourbigou, L. Magna, and L. Saussine from IFP for fruitful discussions.

Supporting Information Available: The isoelectron density surfaces for catalysts **1**, **5**, and **6** are available free of charge via the Internet at http://pubs.acs.org.

OM800326R